Rodrigues-Ferreira et al. Improving breast cancer sensitivity to paclitaxel by increasing aneuploidy : Supporting Informations

Supporting informations Materials and Methods

Patients and samples

The phase II randomized REMAGUS-02 (R02) trial was described elsewhere (1). Trial and ancillary studies were reviewed by the French Ethics Committee of Bicêtre (CPP IDF VII), ISRCTN 10059974, no. 03-55, 14th October 2004, in compliance with the Helsinki Declaration. All patients were informed and prospectively gave their signed consent to participate in the trial and ancillary studies. Only patients (n=115) who received four cycles of epirubicin (75mg/m^2) and cyclophosphamide (750mg/m^2) followed by four cycles of docetaxel (100mg/m^2) without celecoxib nor trastuzumab (arms B and D) were included in this study. RNA extraction and profiling on Affymetrix U133 Plus 2.0 GeneChips, as well as microarray data normalization were performed as described (1, 2). The M.D. Anderson (MDA) breast carcinoma cohort of patients treated with neoadjuvant chemotherapy was described previously (3). This study was approved by the institutional review boards of MDACC and INEN. All patients signed an informed consent for voluntary participation. All patients (n=133) received weekly paclitaxel and Fluorouracil-Doxorubicin-Cyclophosphamide chemotherapy. Phase III randomized multicenter REMAGUS-04 (R04) trial (NCT01180335) included 142 *HER2*-negative breast cancer patients treated in neoadjuvant settings by either 4 cycles of FEC (Fluorouracil, Epirubicin, Cyclophosphamide) followed by 4 cycles of Docetaxel, weekly Paclitaxel followed by 4 cycles of FEC, or a combination of Docetaxel and Xeloda. All patients were informed and prospectively gave their signed consent to participate in the trial and ancillary studies. This study was approved by French ethics committee of Paris-Bicêtre. Clinical data for the patients of all three cohorts are presented in Supporting dataset **Table S6**. Pathological complete response (pCR) of tumors to treatment was defined according to Chevallier‘s criteria (4) as absence of residual invasive carcinoma in the breast and axillary nodes. Gene profiling for a series of 88 infiltrating ductal primary breast carcinomas from the Institut Curie (Paris, France) designated the Curie Cohort and clinical data for the patients are described elsewhere (5-7). This study was approved by institutional review boards of Institut Curie and all patients have signed written informed consent (7). Ploidy status (aneuploidy, diploidy or multiploidy) was assessed for each tumor by a pathologist.

Real-time RT-PCR analyses

For analysis of samples from the R02 cohort of patients, frozen sections of biopsies dedicated to RNA extraction were prepared by breast pathologists and were processed under RNAse-free conditions (2). Tumor cellularity was evaluated and only biopsies with more than 30% invasive epithelial tumor cells were analysed. Total RNA was extracted from biopsies using a TRIzol method. Quantitative PCR analysis was performed on 6.25 ng cDNA in duplicate. A 5 µL diluted sample of cDNA (6.25ng) was added to 10 µL of the PCR mix. The thermal cycling conditions comprised an initial denaturation step at 95°C for 10 min, 45 cycles at 95°C for 15 sec, and annealing temperature at 60°C for 1 min. All PCR reactions were performed using the ABI Prism 7900 Sequence Detection System (Applied Biosystems Inc., Forster City, USA). The PCR Core reagent kit was used for systems with Taqman probes (Eurogentec, Liège, Belgium). Primers and fluorescent probes for ATIP3a and ATIP3b were designed from published sequences using Primer express software (Applied Biosystems Inc.). BLASTN searches against dbEST and nr (the non-redundant set of the GenBank sequence database) were performed to confirm the total gene specificity of the chosen nucleotide sequences and the absence of DNA polymorphisms. Primers and probes for ATIP3a (F:TGCTTTGGATTTAGGAAGTGGTCTAG; R :GATCGAGCCGTATCTCCTCAGA; P :AACTGGACACACGCCTG), ATIP3b (F :CAGTGCTGATCGAGCCGTATC; R :GCGGCATTACCAGCAGAACT; P :CTCAGAGGATCAGGCG) and *MTUS1* (*Hs01001516*) were obtained from Thermofischer Scientific. TATA Box binding protein (TBP) was used as endogenous reference gene (2). Human breast cancer cell lines cDNA were used to generate 8 points standard curves for each pair of primers. Target quantities were normalized to the reference gene and calibrated using the second point of each standard curve. Final results were expressed as N-fold differences in target gene expression relative to the reference genes and the calibrator and are expressed as:

$$E_{\text{target}}^{(Ct\ \text{calibrator} - Ct\ \text{sample})} / E_{\text{reference gene}}^{(Ct\ \text{calibrator} - Ct\ \text{sample})},$$

where E is the efficiency of PCR measured using the slope of the calibration curve, and Ct is the cycle threshold. No Reverse-transcription Controls (NTC) were included in each batch of samples.

Patient-derived xenografts

Patient-derived xenografts were established from early stage breast cancers as previously described (8). HBCx-12A, HBCx-12B and HBCx-39 were established from residual tumors after neo-adjuvant chemotherapy. Breast cancer fragments were obtained from patients at the time of surgery, with informed written patient consent. The experimental protocol was done according to French regulations and was approved by the institutional review boards of the Institut Curie (8). For therapeutic assays, human breast cancer xenografts (HBCx) were transplanted into female 8-week-old Swiss nude mice. When tumors reached a volume of 60-200 mm3, mice were treated by a combination of Adriamycin (2mg/kg) and Cyclophosphamide (100mg/kg) or by Docetaxel (20mg/kg). Tumor growth inhibition was calculated as the ratio of the mean of tumor volume in treated group and the mean of tumor volume in control group. Tumors showing more than 50% growth inhibition were considered sensitive (S) whereas those with less than 50% inhibition were considered resistant (R).

RNA extraction and reverse transcription were performed as previously described (8). cDNA (5 ng) was used for real-time PCR analysis using Fast Start SYBR Green I reagent (Roche) and LightCycler instrument. ATIP3-specific primers on exons 2 and 4 were used (F: GGCGGAACAGTGACAATA; R: GCAAATTCACCCATGACGA). Each reaction was carried out in duplicate. EEF1G cDNAs served as internal controls, as previously described (5). Results are expressed relative to EEF1G values.

Antibodies and reagents

Antibodies directed against alpha-tubulin (DM1A) and Vinculin (hVIN-1) were from Sigma, anti-PARP was from Cell Signaling, anti-Pericentrin was from Abcam and anti-MTUS1 was from Aviva. Anti-Caspase3 (3G2) were from Cell Signaling, anti-Mcl-1 (S19) was from Santa Cruz. Paclitaxel (PTX), Docetaxel (DTX) and Doxorubicin were purchased from Sigma-Aldrich.

Immunohistochemistry

Immunohistochemistry was performed on 5 µm sections from formalin-fixed, paraffin-embedded breast cancer xenograft (HBx) tissue microarray (TMA). Antigen retrieval and immunostaining with anti-MTUS1 antibody (Aviva) were performed as previously described (5). MTUS1 immunoreactivity in TMA sections was scored based on the percentage of positive cells and the intensity (1 to 3) of the staining.

Cells

HCC1143 breast cancer cells and HCT116 colon cancer cells were purchased from American Type Culture Collection (ATCC). SUM52-PE breast cancer cells were a kind gift of Dr N. Turner (London, UK) (9). MDA-MB-231-Luc-D3H2LN breast cancer cells (designated MDA-MB-231) obtained from Caliper Life Science (Xenogen) were derived from an *in vivo* selected metastatic subclone of MDA-MB-231 cells expressing luciferase and were grown as described (10). HeLa and HeLa-mCherryH2B cells were described previously (5, 6).

Multicellular spheroids (MCS)

SUM52-PE breast cancer cells (2,000) were seeded in 96-well plate round bottom coated with Polyhema (Poly2-hydroxyethylmethacrylate, Santa Cruz) to prevent cell adhesion. After centrifugation for 5 min at 1200 rpm, cells were allowed to grow in complete medium. Multicellular tumor spheroids (MCS) were formed after 3 days.

For viability assay, MCS were treated with various doses of Paclitaxel (PTX), Docetaxel (DTX) or Doxorubicin (DOXO) for 3 to 6 days. Viability was determined by measuring MCS area using the ImageJ software and confirmed by measurement of ATP using ATPlite assay (Perkin Elmer) or by metabolic activity using Alamar blue assay.

TUNEL assay

Apoptotic cells in MCS were detected by TUNEL assay using *in situ* cell death detection kit (Roche) according to manufacturer's protocol. Briefly, MCS were fixed for 30 min in paraformaldehyde 4% and permeabilized in citrate buffer 0.5% triton-X100 for another 30 min. After 3 washes in PBS, the MCS were incubated with TUNEL TdT enzyme reaction mixture at 37°C for 2 hrs. DAPI was used to stain DNA. TUNEL-positive cells were visualized and photographed with Leica SPE confocal microscope. The number of TUNEL-positive cells was counted using ImageJ software.

Apoptosis by flow cytometry

HeLa cells transfected for 48hrs with control-siRNA or ATIP3-specific-siRNA were treated with PTX (5nM) for 18hrs prior staining with annexin-V FITC/propidium iodide. Cells were analyzed using BD LRS Fortessa cytometer.

Confocal microscopy

For analysis of mitotic index in 3D models, SUM52PE MCS stably silenced or not for ATIP3 were treated for 3 days with 50nM PTX, then fixed in 4% paraformaldehyde and incubated with mouse anti-alpha-tubulin (DMA1, Sigma) and anti-pericentrin antibodies (Abcam). Nuclei were stained with DAPI. Imaging was performed using a Leica SPE confocal microscope with 63X oil objective. The number of mitotic cells relative to total nuclei was counted in 3 to 6 MCS using ImageJ software.

For quantification of centrioles, HeLa cells were transfected for 48 hrs with control-siRNA (20nM) or ATIP3-specific-siRNA (20nM) (sens strand UGG CAG AGG UUU AAG GUU A, Dharmacon, ThermoFisher Scientific) using Lipofectamine 2000 (Invitrogen), and treated with PTX (5 nM) during 18 hrs. Cells were then fixed with ice-cold methanol and incubated with anti-pericentrin (Abcam) and anti-centrin (clone 20H5, Millipore) antibodies. Imaging was performed using a Leica SP8 confocal microscope with 63X oil objective.

Live cell imaging

For live cell imaging, HeLa-mCherryH2B cells were transfected for 48hrs with control-siRNA or ATIP3-specific-siRNA and incubated with sir-Tub (2.5nM) prior treatment with PTX (2nM). Cells were imaged on a confocal laser scanning microscope multiphoton TCS SP8 MP (Leica) objx40, every 8 min for 66hrs. Multi-dimensional acquisitions were performed in time-lapse mode using ICy software. Image analysis was performed using ImageJ software.

Quantification of mitotic defects

For quantification of mitotic abnormalities, HeLa cells were transfected for 72 hrs with control-siRNA (20nM) or ATIP3-specific-siRNA (20nM) (sens strand UGG CAG AGG UUU AAG GUU A, Dharmacon, ThermoFisher Scientific) using Lipofectamine 2000 (Invitrogen), and treated with DMSO or PTX (2 nM) during 6 hrs. Transfected cells were fixed with ice-cold methanol and incubated with anti-alpha-tubulin and anti-pericentrin antibodies. Imaging was performed using a Leica SPE confocal microscope with 40X oil objective.

Analysis of mitotic defects was performed on all mitotic cells from 5 to 6 pictures - each containing 20 to 60 cells - of 3 independent experiments. Mitotic cells containing more than two spindle poles (based on tubulin and pericentrin staining) were defined as

multipolar. The number of spindle poles per mitotic cells was determined by tubulin and pericentrin staining. An acentrosomal pole was defined as a spindle pole stained by tubulin but with no pericentrin staining. Centrosome amplification was determined by the presence of more than 2 centrosomes per mitotic cell. Number of centrosomes per mitotic cell was quantified based on pericentrin staining.

DNA content analysis and chromosome spread

For DNA content analysis, HeLa cells were transfected for 48 hrs with control-siRNA or ATIP3-specific-siRNA and treated with PTX (5 nM) during 18 hrs. Cells were then fixed with ice-cold ethanol and resuspended in PI solution (propidium iodide 10 µg/ml, RNAse A 50µg/ml) 30min at 37°C, then analyzed using using BD LSR Fortessa cytometer. The cell cycle distribution was determined using DiVa software."

For chromosome number measurement, HCT116 cells were transfected for 48hrs with control-siRNA or ATIP3-specific siRNA and treated with PTX (5nM) during 18hrs. Harvested cells were resuspended in KCl buffer (75mM) and incubated for 15min at 37°C. After centrifugation, the cells were fixed 3 times with methanol/ Acid Acetic buffer (3:1) for 30 min. Cells were then dropped onto coverslips and stained with DAPI.

Statistical analysis

Statistical analyses were done using JMP-7 and GraphPad Prism6 softwares. The association between clinicopathological characteristics and pathological response after neoadjuvant chemotherapy were calculated using the chi-squared and the Fisher exact tests. The association between pathological response and multiple biomarkers was evaluated by a logistic regression model using categorical and continuous variables. Dot plot analyses were done using Mann–Whitney test. Data in bar graphs (mean +/− SD) were analyzed using 2-tail unpaired Student *t* test. $P < 0.05$ was considered statistically significant.

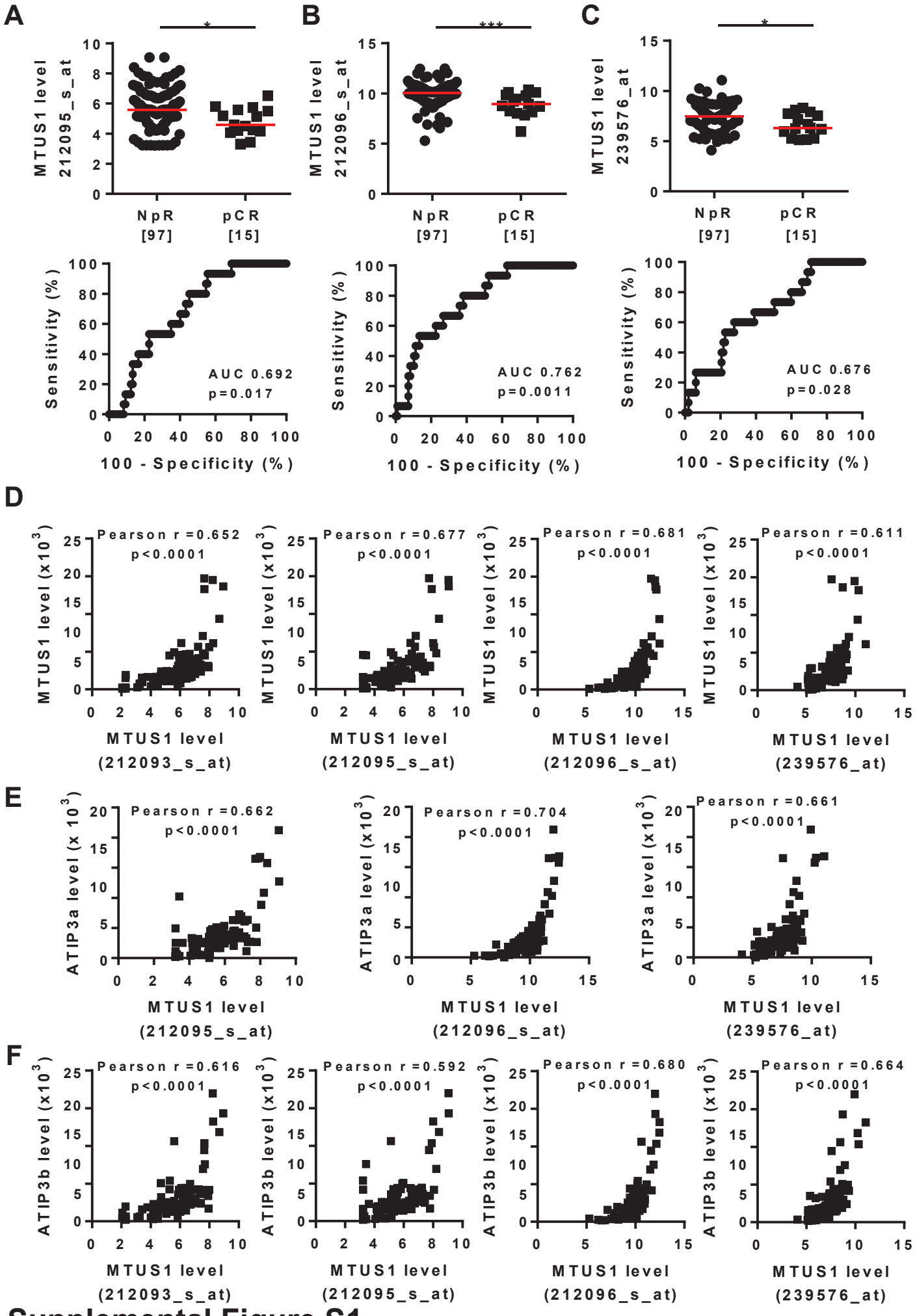

Supplemental Figure S1

Supporting dataset Figure S1. Low levels of *MTUS1* predict response to neoadjuvant chemotherapy in the REMAGUS02 (R02) cohort

A- Upper: Scattered dot plot of *MTUS1* probeset intensity (212095_s_at) in tumors from 115 patients of the R02 cohort with no pathological response (NpR) or achieving pathological complete response (pCR) after neoadjuvant chemotherapy. Numbers of samples are indicated under brackets.

Lower: ROC curve evaluating the performance of *MTUS1* expression for predicting complete response to neoadjuvant chemotherapy. AUC Area Under the Curve.

B- Same as A, with *MTUS1* probeset 212096_s_at.

C- Same as A and B, with *MTUS1* probeset 239576_at.

D- Correlation between *MTUS1* (212093_s_at, 212095_s_at, 212096_s_at, 239576_at) probeset intensities and *MTUS1* transcripts levels measured by real-time RT-PCR using oligonucleotides located in 3' exons of the gene, in 106 breast tumor samples of the R02 cohort.

E- Same as D, using oligonucleotides designed in 5' exons that are specific to ATIP3a transcripts.

F- Same as D and E, using oligonucleotides designed in 5' exons that are specific to ATIP3b transcripts.

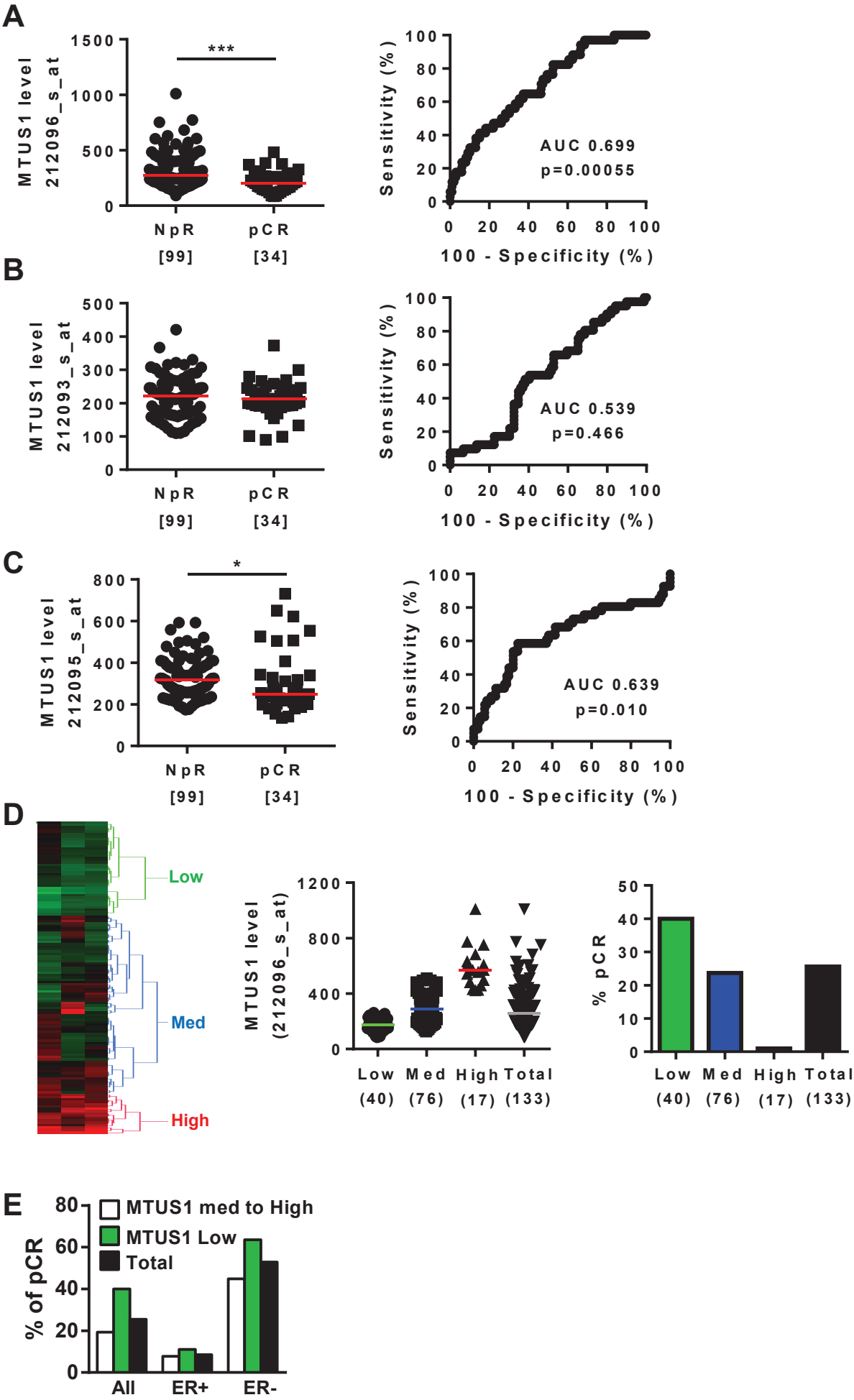

Supplemental Figure S2

Supporting dataset Figure S2. Low levels of *MTUS1* predict response to neoadjuvant chemotherapy in the M.D. Anderson (MDA) cohort

A- Left: Scattered dot plot of *MTUS1* probeset (212096_s_at) intensity in tumors from 133 patients of the MDA cohort with no pathological response (NpR) or achieving pathological complete response (pCR) after neoadjuvant chemotherapy. Numbers of samples are indicated under brackets.

Right: ROC curve evaluating the performance of MTUS1 expression for predicting complete response to neoadjuvant chemotherapy. AUC Area Under the Curve

B- Same as A, with *MTUS1* probeset 212093_s_at.

C- Same as A and B, with *MTUS1* probeset 212095_s_at.

D- Left: Heat map and hierarchical clustering of 133 breast tumor samples based on the intensities of *MTUS1* (212096_s_at; 212093_s_at; 212095_s_at) probesets. Heat map illustrates relative expression profiles of *MTUS1* (column) for each tumor sample (line) in continuous color scale from low (green) to high (red) expression. Dendogram of the 3 selected tumor groups is shown on the right.

Middle: Scattered dot plot of *MTUS1* expression in each of the 3 selected clusters based on the dendogram on the left. Numbers of samples are under brackets.

Right: Proportion of patients with pCR according to *MTUS1* level in each selected cluster. Numbers of tumors in each group are indicated under brackets.

E- Proportion of patients with pCR according to *MTUS1* level in all tumors (All) and in ER+ and ER- tumors. Numbers of tumors in each group are indicated under brackets.

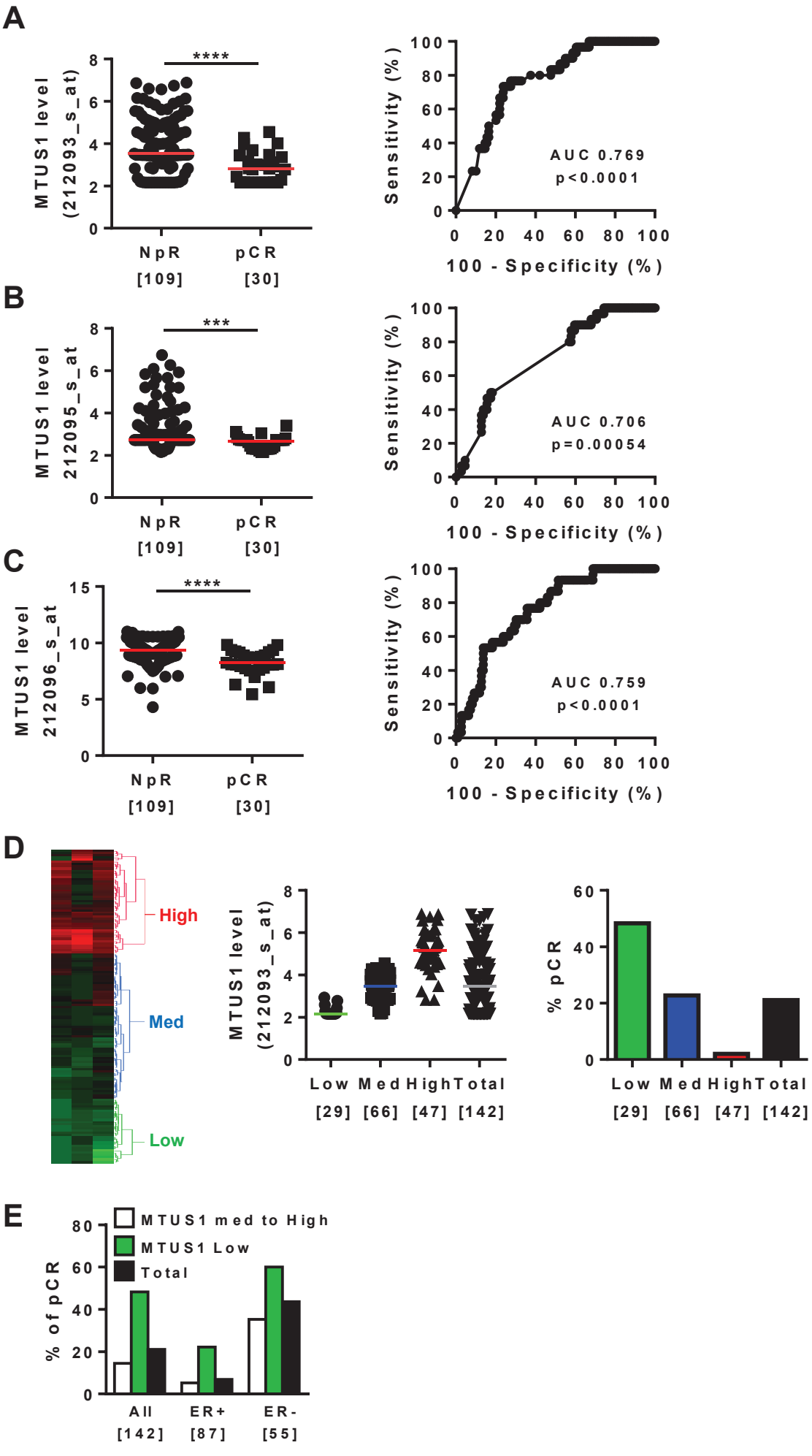

Supplemental Figure S3

Supporting dataset Figure S3. Low levels of *MTUS1* predict response to neoadjuvant chemotherapy in the REMAGUS04 (R04) cohort

A- Left-Scattered dot plot of *MTUS1* expression (probeset 212093_s_at) in tumors from 139 patients of the R04 cohort with no pathological response (NpR) or achieving pathological complete response (pCR) after neoadjuvant chemotherapy. Numbers of samples are indicated under brackets.

Right- ROC curve evaluating the performance of *MTUS1* expression for predicting complete response to neoadjuvant chemotherapy. AUC Area Under the Curve

B- Same as A, with *MTUS1* probeset 212095_s_at.

C- Same as A and B, with *MTUS1* probeset 212096_s_at.

D- Left- Heat map and hierarchical clustering of 142 breast tumor samples based on the intensities of *MTUS1* (212096_s_at; 212093_s_at; 212095_s_at) probesets. Heat map illustrates relative expression profiles of *MTUS1* (column) for each tumor sample (line) in continuous color scale from low (green) to high (red) expression. Dendogram of the 3 selected tumor groups is shown on the right.

Middle- Scattered dot plot of *MTUS1* expression in each of the 3 selected clusters based on the dendogram on the left. Numbers of samples are under brackets.

Right- Proportion of patients with pCR according to *MTUS1* level in each selected cluster. Numbers of tumors in each group are indicated under brackets

E- Proportion of patients with pCR according to *MTUS1* level in all tumors (All) and in ER+ and ER- tumors. Numbers of tumors in each group are indicated under brackets.

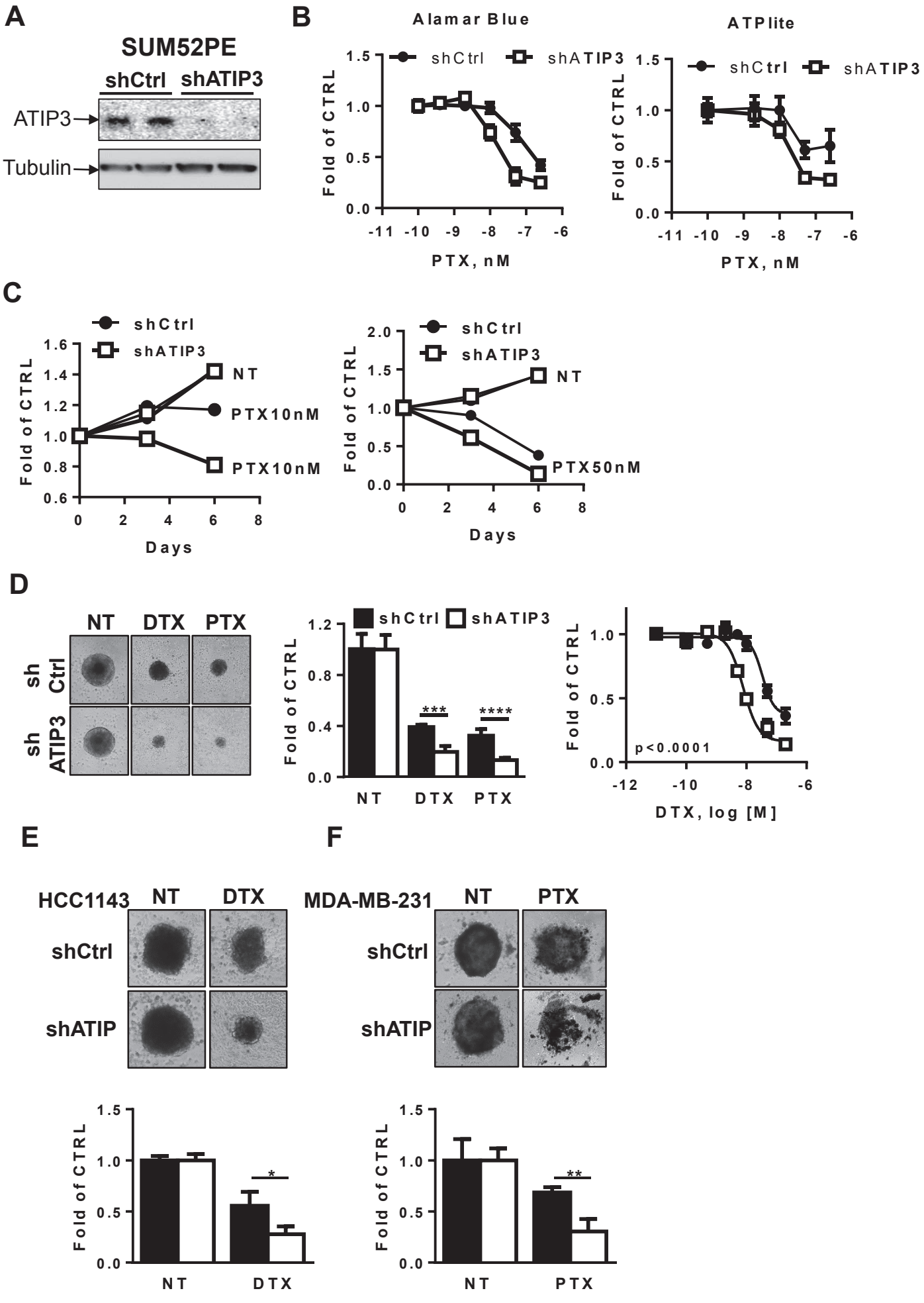

Supplemental Figure S4

Supporting dataset Figure S4. ATIP3 silencing sensitizes breast cancer multicellular spheroids (MCS) to taxanes.

A- Western Blot analysis of ATIP3 expression in SUM52PE cells silenced (shATIP3) or not (shCtrl) for ATIP3. Tubulin is used as internal loading control.

B- Dose response curves of SUM52PE MCS expressing (shCtrl) or not (shATIP3) ATIP3 and treated for 3 days with increasing concentrations of Paclitaxel (PTX). MCS viability is quantified by mitochondrial enzyme activity (Alamar Blue, Left panel) and by ATP measurement (ATPlite, Right panel).

C- Growth curves of SUM52PE MCS expressing (shCtrl) or not (shATIP3) ATIP3 and treated with 10nM (Left panel) or 50nM (Right panel) PTX.

D- SUM52PE spheroids expressing (shCtrl) or not (shATIP3) ATIP3 were treated for 6 days with 50nM Docetaxel (DTX) or Paclitaxel (PTX) and photographed (Left panel). Picture represents one spheroid of the quadruplicate. Spheroid area plotted in the histogram (Middle panel). ****$p<0.0001$. Right panel : Dose response curve of SUM52PE spheroids expressing (shCtrl) or not (shATIP3) ATIP3 and treated for 6 days with increasing concentrations of Docetaxel (DTX).

E- HCC1143 MCS expressing (shCtrl) or not (shATIP3) ATIP3 were treated for 6 days with 50nM Docetaxel (DTX) and photographed. Shown is one MCS of the quadruplicate. MCS area were measured and results are plotted in the histogram below. *$p<0.05$.

F- Same as D, for MDA-MB-231 MCS treated with PTX. **$p<0.01$.

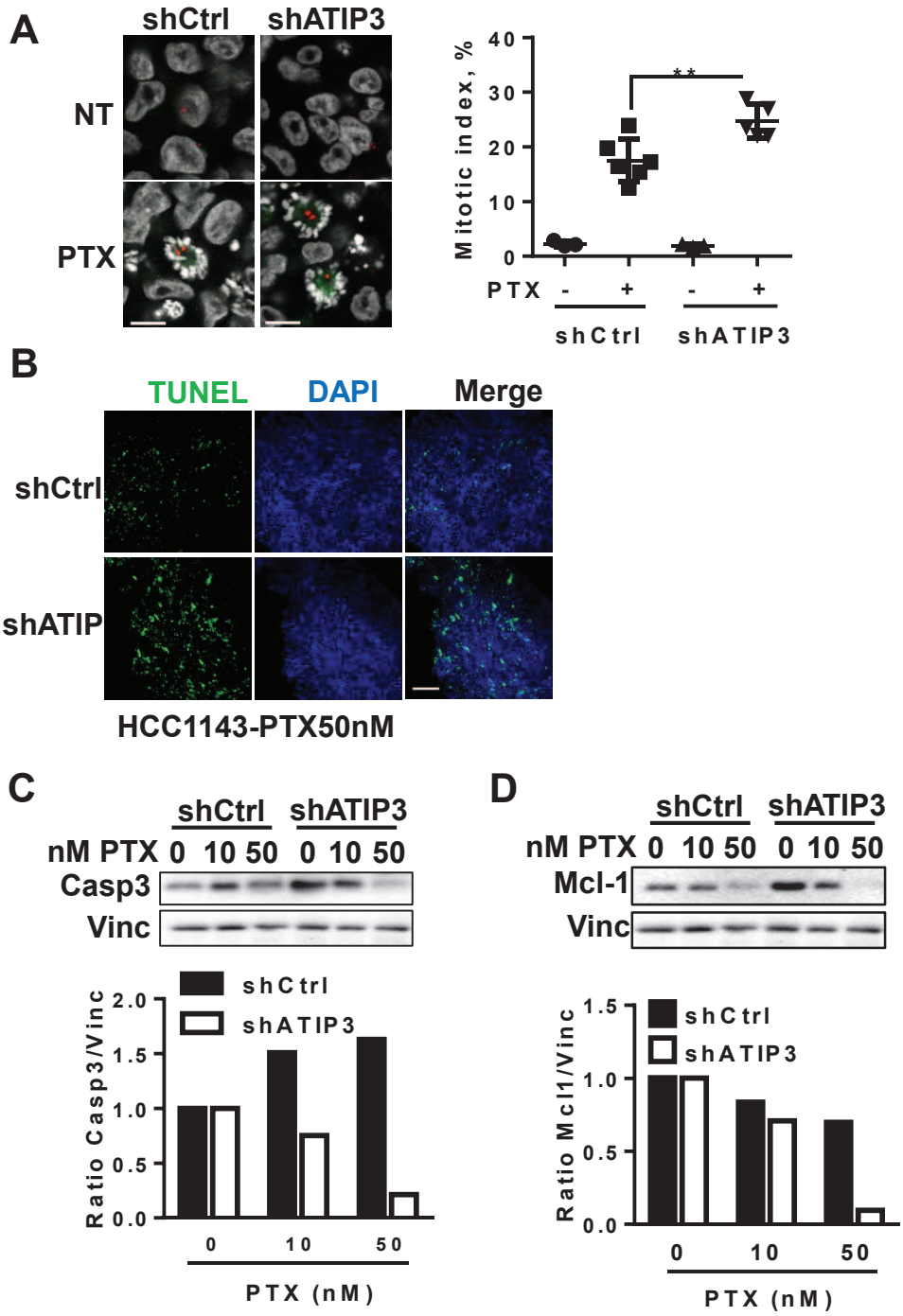

Supporting dataset Figure S5. ATIP3 silencing increases PTX effect on mitotic arrest and apoptosis

A- Photographs illustrating increased mitotic index upon treatment of SUM52PE MCS for 72hrs with PTX (50 nM). DNA is stained by DAPI (grey) and centrosomes (red) are stained with antibodies directed against pericentin. Quantification is shown on the Right. Obj x63, scale bar 10µm. **p<0.01

B- Representative photographs of HCC1143 MCS expressing (shCtrl) or not (shATIP) ATIP3 and treated with 50nM of PTX prior to staining with TUNEL reagent (green) and DAPI (blue). Obj x20, scale bar 100µm.

C- Western-Blot analysis of Caspase 3 (Casp3) in MCS expressing (shCtrl) or not (shATIP3) ATIP3 treated with 10 and 50nM of PTX. Vinculin (Vinc) is used as internal loading control. Lower panel: quantification of Casp3 intensity relative to Vinc and normalized to the condition without PTX. Shown is one representative experiment out of 4.

D- Same as C, using antibodies against Mcl-1.

Supplemental Figure S5

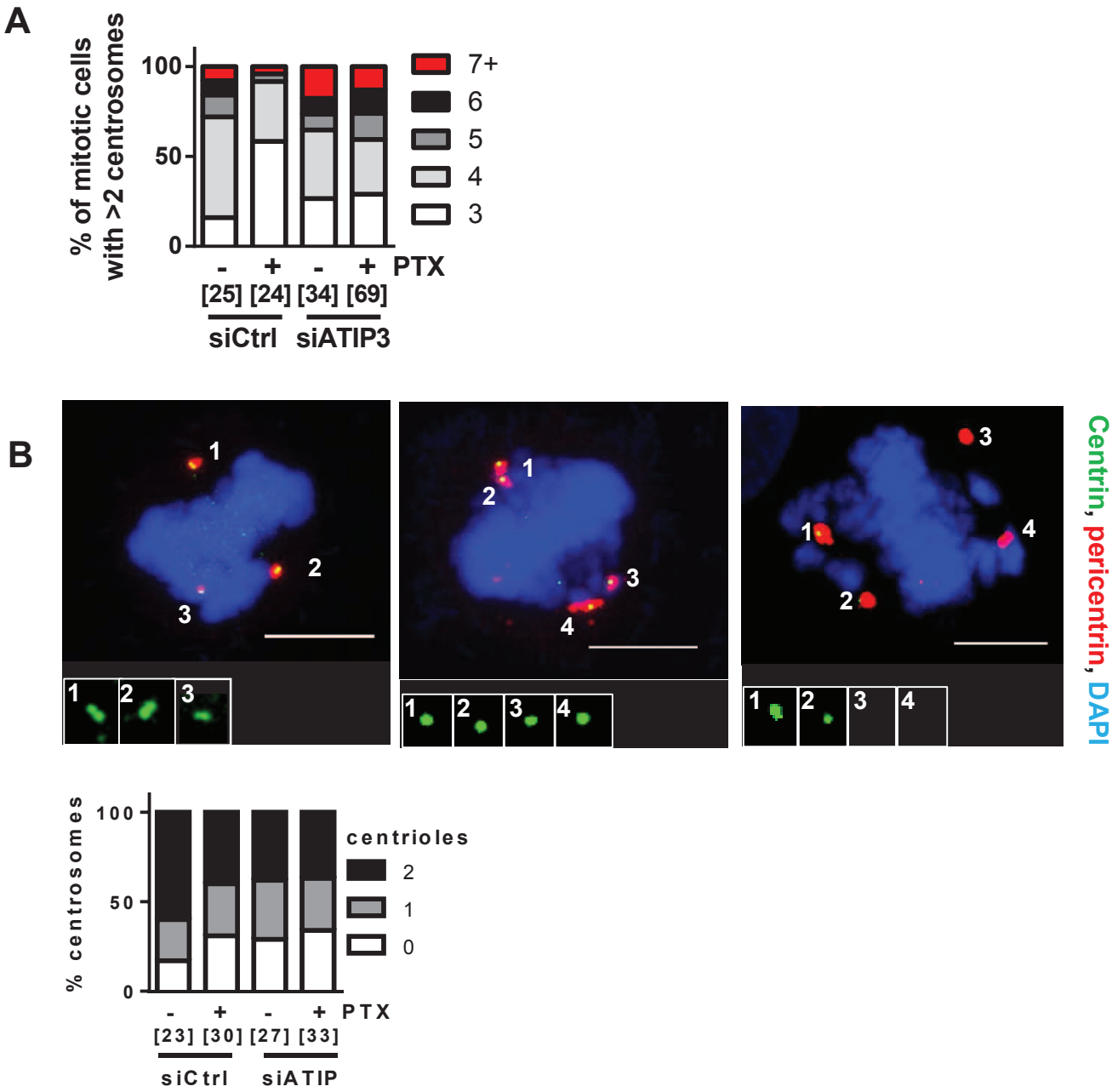

Supporting dataset Figure S6. ATIP3 silencing induces centrosome abnormalities
A- Proportion of mitotic HeLa cells with abnormal number of spindle poles upon 48 hrs ATIP3 silencing and 18hrs PTX (2nM) treatment.
B- Photographs illustrating abnormal centrosomes in mitotic HeLa cells expressing (shCtrl) or not (shATIP) ATIP3 and treated with 2nM of PTX for 18 hrs. Cells were stained with DAPI (blue) and with antibodies directed against pericentin (red) and centrin (green). Inserts illustrate centrosomes containing 2, 1 or no centriole. Quantification is shown below. Obj x63, scale bar 10µm.

Supplemental Figure S6

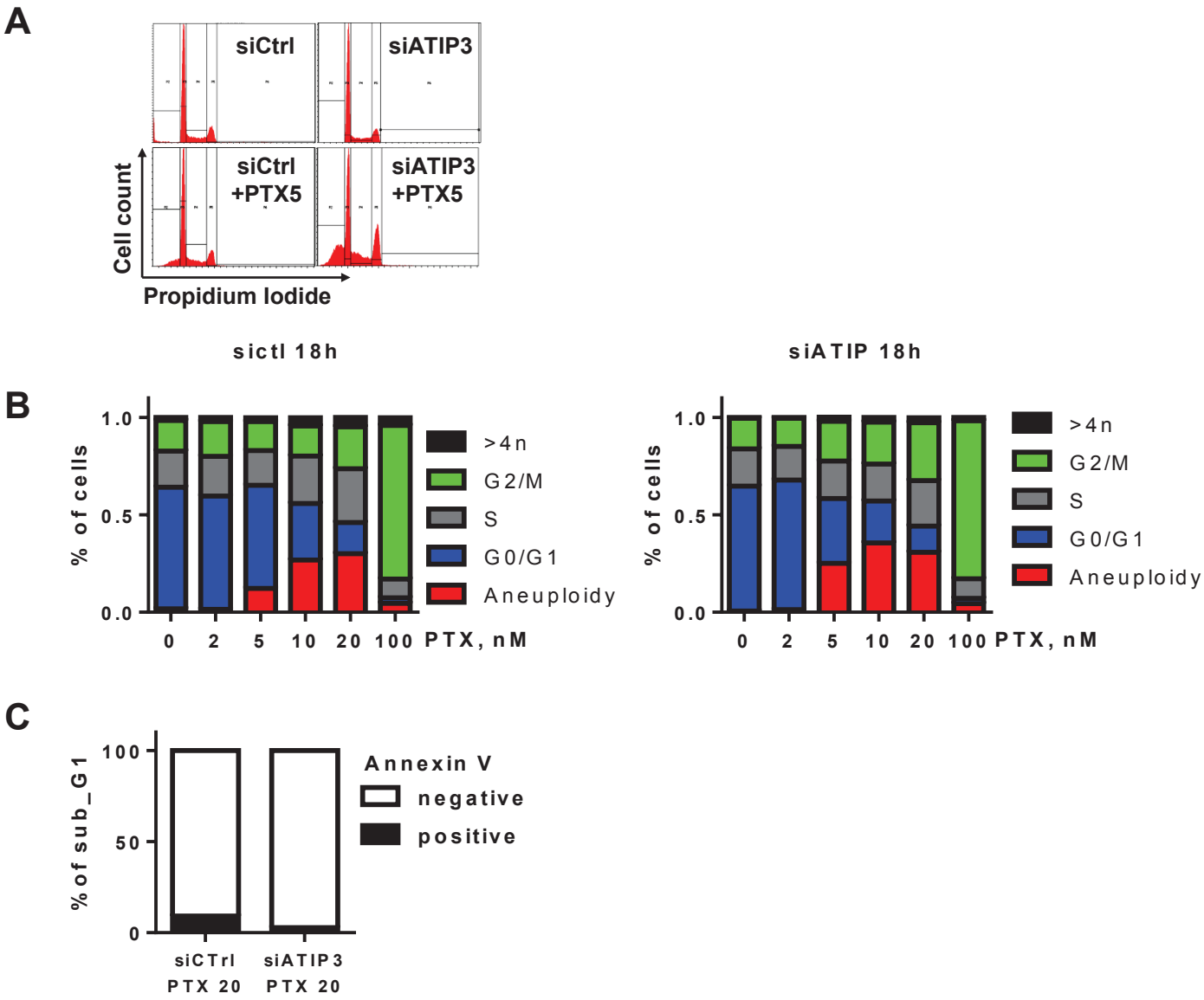

Supporting dataset Figure S7. ATIP3 silencing induces aneuploidy

A- FACS analysis of DNA content of HeLa cells transfected with scramble or ATIP3-directed siRNA, treated or not with 5nM PTX for 18h.

B- FACS analysis of DNA content of HeLa cells transfected with scramble siRNA (Left panel) or ATIP3-directed siRNA (Right panel) and treated for 18h with increasing doses of PTX as indicated. Shown is the proportion of cells in each cell cycle fraction.

C- Proportion of sub_G1 (hypodiploid) cells stained with Annexin V among HeLa cells transfected with scramble or ATIP3-directed siRNA and treated for 18h with 20 nM PTX.

Supplemental Figure S7

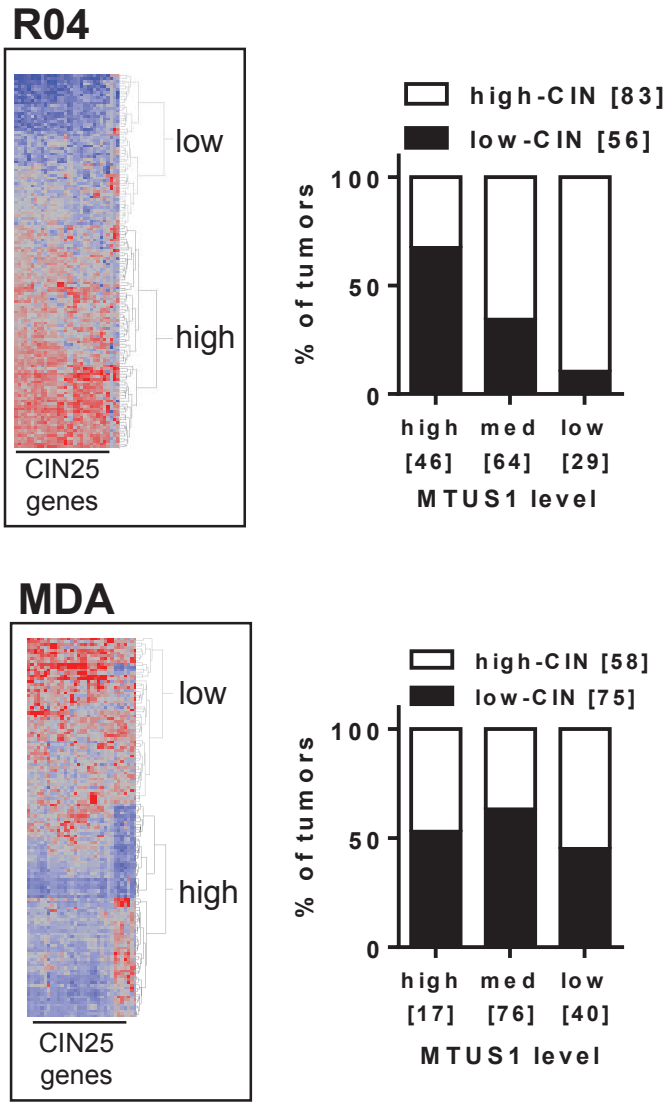

Supporting dataset Figure S8. ATIP3 silencing induces aneuploidy
Heatmap and hierarchical clustering of breast tumor samples from the R04 (Upper panel) and M.D. Anderson (Lower panel) studies, based on the intensities of the 25 genes from chromosomal Instability CIN signature. Proportion of tumors expressing high level (high-CIN) or low levels (low-CIN) of CIN signature according to ATIP3 levels are shown on the right. Number of tumors is indicated under brackets.

Supplemental Figure S8

Legends to Supporting dataset Tables

Supporting dataset Table S1. MT-regulating genes analyzed according to their probeset expression values in sensitive (pCR) and resistant (NpR) tumors from patients included in the REMAGUS02 (R02, Table S1A), M.D. Anderson (MDA, Table S1B), and REMAGUS04 (R04, Table S1C) studies. The 280 MT-regulating genes were selected from a litterature search combined with Ingenuity Pathway Analysis (IPA) of the network of genes connected to tubulin and EB1.

Supporting dataset Table S2. MT-regulating genes differentially expressed between sensitive (pCR) and resistant (NpR) tumors from patients included in the REMAGUS02 (R02, left), M.D. Anderson (MDA, middle), and REMAGUS04 (R04, right) studies. Genes up-regulated in pCR are in yellow. Genes down regulated in pCR are in blue.

Supporting dataset Table S3. Univariate and multivariate analysis of predictive factors of pathological complete response (pCR) in the M.D. Anderson (MDA) and REMAGUS04 (R04) studies.

Supporting dataset Table S4. Characteristics of Patients-derived Xenografts used in this study, including ATIP3 level determined by qPCR and Immunohistochemistry (IHC score), and response to Docetaxel (DTX) and Anthracycline plus Cyclophosphamide (AC).

Supporting dataset Table S5. *MTUS1* level and ploidy status in breast tumors from the Curie cohort. The intensities of four *MTUS1* probesets (212096_s_at; 212093_s_at; 212095_s_at 239576_at) were used to determine *MTUS1* level.

Supporting dataset Table S6 Clinical information of the patients included in the REMAGUS02 (R02, left), M.D. Anderson (MDA, middle) and REMAGUS04 (R04, right) studies.

Legends to Supporting dataset Videos

Movie 1. Time-lapse videomicroscopy of cell division in HeLa-mChH2B cells transfected with scramble siRNA (siCtrl)

Movie 2. Time-lapse videomicroscopy of cell division in HeLa-mChH2B cells silenced for ATIP3 by transfection with siRNA (siATIP3)

Movie 3. Time-lapse videomicroscopy of cell division in HeLa-mChH2B cells transfected with scramble siRNA (siCtrl) and treated with 2 nM PTX.

Movie 4. Time-lapse videomicroscopy of cell division in HeLa-mChH2B cells silenced for ATIP3 by transfection with siRNA (siATIP3) and treated with 2 nM PTX.

Supporting Informations References

1. Valet F, de Cremoux P, Spyratos F, Servant N, Dujaric ME, Gentien D, et al. Challenging single- and multi-probesets gene expression signatures of pathological complete response to neoadjuvant chemotherapy in breast cancer: Experience of the REMAGUS 02 phase II trial. *The Breast*. **22**, 1052–1059 (2013).
2. de Cremoux P, Valet F, Gentien D, Lehmann-Che J, Scott V, Tran-Perennou C, et al. Importance of pre-analytical steps for transcriptome and RT-qPCR analyses in the context of the phase II randomised multicentre trial REMAGUS02 of neoadjuvant chemotherapy in breast cancer patients. *BMC Cancer.***11**, 215-224 (2011).
3. Hess KR, Anderson K, Symmans WF, Valero V, Ibrahim N, Mejia JA, et al. Pharmacogenomic predictor of sensitivity to preoperative chemotherapy with paclitaxel and fluorouracil, doxorubicin, and cyclophosphamide in breast cancer. *J Clin Oncol*. **24(26),** 4236-44 (2006).
4. Chevallier B, Roche H, Olivier JP, Chollet P, Hurteloup P. Inflammatory breast cancer. Pilot study of intensive induction chemotherapy (FEC-HD) results in a high histologic response rate. *Am J Clin Oncol*.**16**, 223–228 (1993).
5. Rodrigues-Ferreira S, Di Tommaso A, Dimitrov A, Cazaubon S, Gruel N, Colasson H, et al. 8p22 MTUS1 Gene Product ATIP3 Is a Novel Anti-Mitotic Protein Underexpressed in Invasive Breast Carcinoma of Poor Prognosis. *PLoS ONE.* **4**, e7239 (2009).
6. Molina A, Velot L, Ghouinem L, Abdelkarim M, Bouchet BP, Luissint A-C, et al. ATIP3, a Novel Prognostic Marker of Breast Cancer Patient Survival, Limits Cancer Cell Migration and Slows Metastatic Progression by Regulating Microtubule Dynamics. *Cancer Res*. **73**, 2905–2915 (2013).
7. Reyal F, Stransky N, Bernard-Pierrot I, Vincent-Salomon A, de Rycke Y, Elvin P, et al. Visualizing chromosomes as transcriptome correlation maps: evidence of chromosomal domains containing co-expressed genes--a study of 130 invasive ductal breast carcinomas. *Cancer Res.* **65**, 1376-1383 (2005).
8. Marangoni E, Vincent-Salomon A, Auger N, Degeorges A, Assayag F, de Cremoux P, et al. A new model of patient tumor-derived breast cancer xenografts for preclinical assays. *Clin Cancer Res*. **13**, 3989–3998 (2007).
9. Turner N, Lambros MB, Horlings HM, Pearson A, Sharpe R, Natrajan R, et al. Integrative molecular profiling of triple negative breast cancers identifies amplicon drivers and potential therapeutic targets. *Oncogene.* **29,** 2013-2023 (2010).

10. Rodrigues-Ferreira S, Abdelkarim M, Dillenburg-Pilla P, Luissint AC, di-Tommaso A, Deshayes F, et al. Angiotensin II facilitates breast cancer cell migration and metastasis. *PLoS ONE.* **7(4),** e35667 (2012).